УДК 621.317

MIROSHNIK M.A., Dr. of tech. science,
KOVALENKO M.A., graduate student (Ukrainian State Academy of Railway Transport),
ZAICHENKO O.B., assistant (Kharkiv National University of Radio Electronics)

Investigation of the influence of generator signal higher order propagation components and ways of its compensating in the multiprobe microwave multimeter

Представил д.т.н. Моисеенко В.И.

The physical and mathematical and metrological model of higher order propagation modes in multiprobe microwave multimeter with three sensors was composed. The higher order propagation modes error estimation, which is proposed, minimizes error by shifting sensors from the middle of the waveguide broad wall to the periphery, without changing the distance between the sensors along the direction of energy propagation through the waveguide.
Key words: *Cryptography, Data Encryption Standard (DES), linear cryptanalysis, FPGA, efficient implementations.*

1. Introduction

Despite the efforts of specialists in the manufacture of generating units, all such devices until now generate not only the useful signal, but also higher order propagation modes [2]. To reduce power level of higher order propagation modes usually use filters [1], but their disadvantage is the high cost and complexity.

The issue of determination of higher order propagation modes spectrum are devoted such fundamental works as [4] (Fig. 1) and [3] Table 1. Fig. 1 shows the relationship between higher order propagation modes for a waveguide section 90x45mm. Table 1 show the quantitative estimation of the spectrum, which will be used in the simulation. Interest in this subject is not weakened, and so far [5] since for great variety of practical applications this problem has great importance. For example, in the process of drying and heating operations, especially practical value has the ability to measure the power of wave types, which will allow creating a uniform distribution of power flux density of the heated object by adjusting the intensity the individual types of waves.

In our view this area is sufficiently investigated, but metrological direction is remained little studied. Meanwhile, there is the prospect of more accurate measurements, in particular, the microwave passing power multiprobe method, which led to interest in this important topic.

As can be seen from Fig. 1 for the second time harmonic modes H20, H01, H11, H30, E11, E21are present.

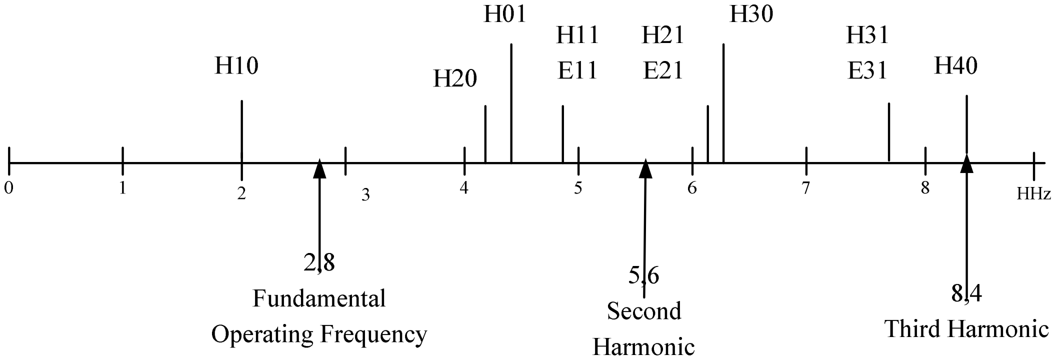

Fig. 1. The critical frequency of the waves in a rectangular waveguide 90x45mm

Table 1

Following harmonic spectrum is typical for M-413 klystron [3]

modes	Fundamental Operating frequency 2856 MHz	Second Harmonic 5712 MHz	Third Harmonic 8568 MHz
H10	31 10	11,206	0,269
H20		1,130	1,490
H01		52,570	0,754
H11		50,643	0,188
E11		8,261	0,450
H21			0,258
E21			0,174
H30			0,138
H31			0,093
E31			0,037
H40			0,042
Total	31 (0 dB)	123,810 (-24 dB)	3,894 (-39 dB)

2. Physical and Mathematical Model of Higher Order Propagation Modes

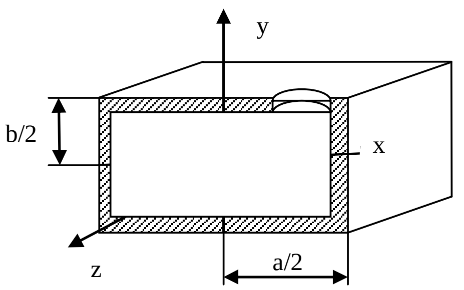

Fig. 2. The coordinate system in a rectangular waveguide

It is proposed a system of coordinates, the origin of that lies on the axis of the waveguide.

As we know the generator stipulates the signal level, frequency range and the presence of harmonics. Mismatched load leads to the appearance of the reflected wave in the microwave tract. The degree of mismatch is quantitatively characterized by modulus Γ and phase φ of complex reflection coefficient of the load. The reflected wave, adding to the incident wave, forms the standing wave in the tract. Thus the higher order propagation modes, the temporal harmonic generator, the standing wave create a complex structure of the field inside the waveguide, and on its walls [4].

The absorbing cylindrical wall of the constantan is used as sensors. This sensor responds to the magnetic field component.

The components of the magnetic field vectors for the wave type H_{mn}, which is distributed in a rectangular waveguide with the center coordinates, which is located on the axis of the waveguide in the direction to the load as shown in Fig. 2 has the following form [8]

$$H_z^+ = H_{mn}\cos\left[\frac{m\pi}{a}\left(x+\frac{a}{2}\right)\right]\cos\left[\frac{n\pi}{b}\left(y+\frac{b}{2}\right)\right]e^{i(\omega\tau-\beta z)}, \tag{1}$$

$$H_x^+ = i\beta\frac{\chi_m}{\chi^2}H_{mn}\sin\left[\frac{m\pi}{a}\left(x+\frac{a}{2}\right)\right]\cos\left[\frac{n\pi}{b}\left(y+\frac{b}{2}\right)\right]e^{i(\omega\tau-\beta z)}, \tag{2}$$

$$H_y^{+} = i\beta \frac{\chi_n}{\chi^2} H_{mn} \sin\left[\frac{m\pi}{a}\left(x+\frac{a}{2}\right)\right]\sin\left[\frac{n\pi}{b}\left(y+\frac{b}{2}\right)\right]e^{i(\omega\tau-\beta z)}. \quad (3)$$

For waves of type E_{mn}

$$H_x^{+} = i\frac{\beta}{Z_E}\frac{\chi_n}{\chi^2} E_{mn} \sin\left[\frac{m\pi}{a}\left(x+\frac{a}{2}\right)\right]\cos\left[\frac{n\pi}{b}\left(y+\frac{b}{2}\right)\right]e^{i(\omega\tau-\beta z)}, \quad (4)$$

$$H_y^{+} = -i\frac{\beta}{Z_E}\frac{\chi_m}{\chi^2} E_{mn} \cos\left[\frac{m\pi}{a}\left(x+\frac{a}{2}\right)\right]\sin\left[\frac{n\pi}{b}\left(y+\frac{b}{2}\right)\right]e^{i(\omega\tau-\beta z)}. \quad (5)$$

We express the coefficients H_{mn} through the incident power in a waveguide of rectangular cross section

$$H_{mn} = \sqrt{\frac{4(2-\delta_{m0}-\delta_{n0})\left(\frac{\chi\lambda}{2\pi}\right)^2 P}{abZ_0\sqrt{1-\left(\frac{\chi\lambda}{2\pi}\right)^2}}}. \quad (6)$$

where δ_{m0}, δ_{n0} – Kroneker-Kapelli symbol

$$\delta_{mn} = \begin{cases} 1, & at \;\; m=n; \\ 0, & at \;\; m \neq n. \end{cases}$$

Similar expression can be obtained for the reflected waves. They differ from the incident wave (1)-(5) by propagation direction (the propagation constant changes its sign to the opposite) and amplitude of the reflected wave is less than incident wave amplitude reflection coefficient Γ times.

For each of the projections the incident wave add reflected wave

$$H_{xmn} = H_x^{+} + H_x^{-},\; H_{ymn} = H_y^{+} + H_y^{-},\; H_{zmn} = H_z^{+} + H_z^{-}.$$

For each mode is written likewise projections on the coordinate axes. According to the principle of superposition field can be represented by the following expression

$$H_x^{\Sigma} = \sum_{mn=1}^{7} H_{xmn},\; H_y^{\Sigma} = \sum_{mn=1}^{7} H_{ymn},\; H_z^{\Sigma} = \sum_{mn=1}^{7} H_{zmn}.$$

The sensor reacts to the magnetic field by heating. The surface density of heat sources

$$Q = \frac{\rho \vec{H}\vec{H}^{*}}{2\Delta},$$

where ρ – specific resistance, Δ – depth of the skin layer,

$$\Delta = \sqrt{\frac{2}{\omega\mu_0\sigma}}.$$

To determine the distribution of heat sources necessary to calculate the scalar product of vectors of the magnetic field on the surface of an absorbing wall. The product is calculated by expression

$$Q = \frac{\rho\left(H_x^{\Sigma}\cdot\left(H_x^{\Sigma}\right)^{*} + H_y^{\Sigma}\cdot\left(H_y^{\Sigma}\right)^{*} + H_z^{\Sigma}\cdot\left(H_z^{\Sigma}\right)^{*}\right)}{2\Delta}.$$

3. Metrological model. Higher order propagation modes error and its minimization

The sensors placed in a certain way in the waveguide usually are used to measure the power in the mismatched tract. The passing power measured with multiprobe multimeter is [7]

$$P_{np} = \sqrt{\frac{1}{3}\left\{(P_1+P_2+P_3)^2 - 2(P_1^2+P_2^2+P_3^2)\right\}},$$

where P_{np} – passing power without regard to higher order propagation modes;

P_i – sensor signal.

Hence, the relative error

$$\delta = \frac{P_{np0} - P_{np}}{P_{np0}} = 1 - \frac{P_{np}}{P_{np0}},$$

where P_{np0} – passing power with higher order propagation modes
or

$$\delta = \frac{H_{10} - \Sigma H_{mn}}{H_{10}} .$$

3.1. Minimization of higher order propagation modes error at a sensor bias

Due to the great complexity of the problem for the three sensors let us fix the position of two sensors in the middle of a broad wall of waveguide, and position of the third sensor varies through waveguide broad wall. According to the simulation results it is recommended to place the sensor offset from the center of broad wall of the waveguide to the periphery, then the higher order propagation modes error is reduced to 0,19 %.

3.2. Minimization of higher order propagation modes error for the two sensors

Let us add yet another mobile sensor. As between the sensor and the error is a complex relationship according to the physical and mathematical models and metrological models let us simulate the movement of both sensors as related events? Fig. 3 depicts the levels of errors, it is evident that the error reaches a minimum at a bias of both sensors from the center to the periphery in the same direction of 0.02 and 0.02 from the center of broad wall and the error is about 0,15 %. Fig. 5 shows a three-dimensional graph, which allows to visualize the behavior of the error depending on the sensor location.

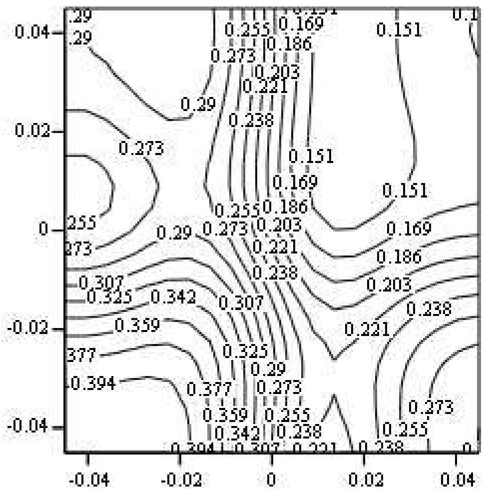

Fig. 3. The level surfaces of higher order propagation modes error

Based on the simulation of the two sensors surface of the response behavior, one can draw conclusion that surface is concave, i.e. there is only one extreme.

3.3. Minimization of higher order propagation modes error for the three sensors

For the three sensors graphical representation is not working, so the error is a function of the position of the three sensors. Therefore, to minimize errors let us use formal methods of optimization, namely, the gradient method of Frank-Wolfe [6]. A typical feature of this problem is that the system of its limits contains only linear equations. So the original nonlinear problem solution can be reduced to solution of linear programming problems. In addition, we make the assumption of the concave nature of the response surface.

As known, when this iterative method is used, at first we find the coordinates of first approximation solution point X, then the gradient is find in the point, then a linear function of the coordinates is built, where the coefficients are taken from the gradient at this point. Then the linear function minimum is determine, it gives the corresponding coordinates of Z. New point is calculated from the following expression.

$$X_{K+1} = X_K + \eta(Z_K - X_K),$$

where X_K – coordinates at к iteration;

Z_K – minimum coordinates;

η – step, the value of which ranges from 0 to 1. The correct choice of the step is very important because it influences the convergence of the algorithm as a whole. The novelty is that it is proposed to calculate the step using a graphical method, which greatly simplifies calculations (Fig. 4). The tools of taking the partial derivative using MathCAD are used. The derivative of the error should be zero. In this figure, the derivative of the error reaches the zero value at $\eta = 0{,}7$.

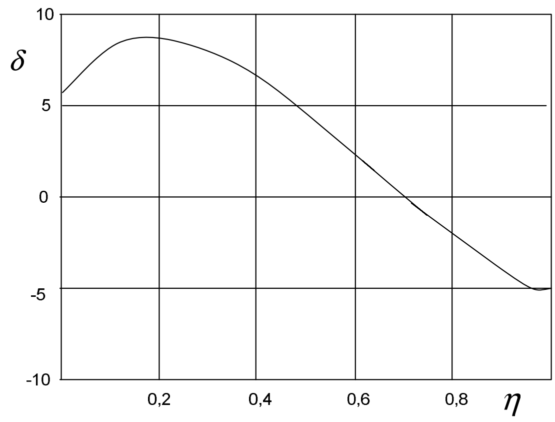

Fig. 4. Determination of the step in the method of Frank-Wolfe

4. Conclusion

Both quantitatively and qualitatively the higher order propagation modes error depending on the position sensor across the wall of waveguide was evaluated in this study. It is at least 11% at the optimal placement of sensors at 0.0225 m from the center to the periphery of the waveguide. The error should be considered as a systematic error remnant. And such result can be explained by the superposition of higher order propagation modes structures.

For the case when takes into account fundamental operating frequency, the second and third harmonics of higher order propagation modes the result are analogous, the method of quantitative evaluation of the error remains same.

References

1 Бецкий О.В., Палатов К.И. Цейтлин М.Б., Ю.Д. Ильин Побочные колебаний в электронных приборах СВЧ Под ред. М. Б. Цейтлина – М.: Радио и связь, 1984. – 152 с.

2 Ребров С.И. Электронная СВЧ-техника. – Электронная техника, Сер.1. СВЧ-техника, вып.1(500), 2009. –. С.31 – 60.

3 Fowkes W.R., Wu E.S. Multimode Harmonic Power Measurement of 40 MW Pulsed S-band Klystrons SLAC-PUB-3396, August, 1984/ Conference of precision Electromagnetic Measurements Dalft, The Netherlands, August 20-24, 1984, pp.1 – 8.

4 M. P. Forrer, K.Tomiyasu . Effect and measurement of harmonics in high power waveguide system 1957, IRE National Convention Record, pt.1, pp.263 – 269.

5 Ивкин П.В. Автореферат Метод измерения проходящей мощности в многомодовых волноводах гальваномагнитными преобразователями Специальность 05.12.07 – «Антенны и устройства микроволновой техники», 2003.

6 Акулинич И.Л. Математическое моделирование в примерах и задачах. Учеб. пособие для студ. М.: Высш школа, 1986. – 319 с.

7 Волков В.М., Зайченко О.Б. Погрешности многозондовых микроволновых мультиметров с эквидистантными датчиками. Український метрологічний журнал. – 2008. – №4. –С.26 – 28.

Мирошник М.А., Коваленко М.А., Зайченко О.Б. Исследование влияния погрешности от
УДК 621.31
внеполосных составляющих генератора в многозондовом микроволновом мультиметре и способы ее компенсации. В данной статье построены физико-математическая и метрологическая модели учета внеполосных составляющих сигнала генератора в многозондовом микроволновом мультиметре с тремя датчиками. Произведена оценка погрешности от внеполосных составляющих сигнала генератора, для минимизации которой предлагается сместить датчики от середины широкой стенки волновода к периферии, не меняя при этом расстояние между датчиками вдоль направления распространения энергии по волноводу.

Ключевые слова: датчик, мультиметр, погрешность, волновод, модель учета, сигнал генератора, внеполосная составляющая, многозондовый микроволновой мультиметр.

Мірошник М.А., Коваленко М.А., Зайченко О.Б. Дослідження впливу похибки від позасмугових складових генератора в багатозондового мікрохвильовому мультиметри і способи її компенсації. У даній статті побудовані фізико-математична і метрологічна моделі обліку позасмугових складових сигналу генератора в багатозондового мікрохвильовому мультиметри з трьома датчиками. Зроблена оцінка похибки від позасмугових складових сигналу генератора, для мінімізації якої пропонується змістити датчики від середини широкої стінки хвилеводу до периферії, не змінюючи при цьому відстань між датчиками уздовж напрямку поширення енергії по хвилеводу.

Ключові слова: датчик, мультиметр, похибка, хвилевід, модель обліку, сигнал генератора, внеполосной складова, багатозондового мікрохвильової мультиметр.

Рецензент д.т.н., профессор, профессор кафедры СКС Листровой С.В. (УкрГАЖТ)

Поступила 27.05.2014 г.